Atorvastatin reduces functional deficits caused by photodynamic therapy in rats

XUGUANG ZHENG[1], MICHAEL CHOPP[1,2], YONG LU[1], JAMES JIANG[1], DANPING ZHAO[1], CHRISTOPHER DING[1], HONGYAN YANG[1], LI ZHANG[1] and FENG JIANG[1]

[1]Department of Neurology, Henry Ford Hospital, Detroit, MI;
[2]Department of Physics, Oakland University, Rochester, MI, USA

Received March 17, 2011; Accepted May 9, 2011

DOI: 10.3892/ijo.2011.1163

Abstract. Clinical studies have indicated that photodynamic therapy (PDT) significantly prolonged the median survival of patients with gliomas. Experimental studies demonstrate that increasing optical energy and photosensitizer dose leads to increased volume of tumor necrosis. However, increasing the light dose delivered to the tumor may increase the risks of inducing permanent neurological deficits. In the current study, we sought to test the behavioral deficits induced in normal rats by brain PDT and the neurorestorative effects of atorvastatin on PDT-induced behavioral deficits. Considering its potential as a combination treatment of brain tumors, we investigated both *in vitro* and *in vivo* whether atorvastatin treatment promotes brain tumor growth. Non-tumored Fischer rats received PDT (n=18). Nine of the PDT-treated animals were treated with atorvastatin. Control animals underwent the same surgical procedure, but did not receive Photofrin and laser light. PDT-treated animals had significant behavioral deficits on Days 2, 5, 7, 9 and 14 after PDT, compared with surgery controls. PDT-treated animals receiving atorvastatin displayed significantly ameliorated behavioral deficits on Days 7, 9 and 14 after PDT, compared to PDT-treated rats. *In vitro* tumor cell viability and growth were evaluated. Atorvastatin did not affect the growth of glioma cells. Fischer rats with intracranial 7-day-old 9L glioma tumor cell implantation were randomly subjected to no treatment, PDT alone, atorvastatin alone, or combined treatment with atorvastatin and PDT (6 rats/group). Our data indicate that atorvastatin did not promote tumor growth in either PDT treated and non-treated rats. However, atorvastatin significantly reduced the cell damage caused by PDT. To further test the mechanisms underlying the atorvastatin-mediated reduction of functional deficits, we investigated the effects of atorvastatin on angiogenesis and synaptogenesis. Our data demonstrate that atorvastatin significantly induced angiogenesis and synaptogenesis in the PDT-damaged brain tissue. Our data indicate that PDT induces functional deficits. Atorvastatin treatment promotes functional restoration after PDT, but does not promote glioma growth *in vitro* and *in vivo*. Atorvastatin reduces astrocyte and endothelial cell damage caused by PDT and induces angiogenesis and synaptogenesis after PDT. Thus consideration and further testing of the combination of atorvastatin and PDT for the treatment of glioma is warranted.

Correspondence to: Dr Feng Jiang, Department of Neurology, Henry Ford Hospital, 2799 West Grand Blvd., Detroit, MI 48202, USA
E-mail: fengj@neuro.hfh.edu

Key words: glioma, photodynamic therapy, functional deficits, atorvastatin

Introduction

Experimental photodynamic therapy (PDT) of cancer has a 100-year history, and for more than 25 years, PDT has been established in the clinical setting as a useful adjuvant to standard treatments for many types of cancer (1,2). Treating solid tumors with PDT involves exposure to tissue-penetrating laser light set at a specific wavelength following systemic administration of a photosensitizing drug, such as Photofrin. However, high dose PDT can also directly damage the surrounding normal brain tissue due to its toxicity and lack of selectivity. PDT induces inflammation, hypoxia, and oxidative stress (3-7). The inflammatory response and oxidative stress induced by PDT stimulate antitumor immunity and an increased response in the brain adjacent to the tumor area raises the possibility of adverse effects including neurological disorders.

Atorvastatin was recently found to improve the functional outcome after stroke (8,9), intracerebral hemorrhage (10), and traumatic brain injury (11-14). There is a body of evidence for the neuroprotective and neurorestorative effects of statins, by enhancing endogenous restorative mechanisms (9-13). In the current study, we evaluated the neuroprotective and neuro-restorative benefits of statin treatment in rats with PDT-induced behavioral deficits.

Materials and methods

Glioma cell culture. 9L, U87, U251n and U87MG cells were kept in a monolayer culture (37˚C, 5% CO_2) in minimum essential media (MEM) with Earle's salts supplemented with 10% fetal bovine serum, 0.2% phenol red and 1% each of L-glutamine, MEM sodium pyruvate, nonessential amino

acids, penicillin, and streptomycin (Gibco, Grand Island, NY). Cells were subcultured and used for implantation when in an exponential phase of growth. To harvest, cells were incubated for 5 min with 0.05% trypsin EDTA (0.53 mM, Gibco), followed by the addition of MEM to make a single cell suspension. This suspension was centrifuged at 1000 rpm (4˚C). The medium was removed and the cells were resuspended in MEM. The cell concentration and viability were determined from a hemacytometer count of a trypan blue dilution and the suspension was diluted with MEM to a concentration of $2x10^7$ cells/ml.

Glioma cell implantation in rats. Six weeks old, Fischer rats were anesthetized with ketamine (80 mg/kg) and xylazine (13 mg/kg) administered intramuscularly (i.m.). Once fixed in a stereotaxic device, the scalp was retracted and the cranium was exposed, and a 3-4 mm incision was made directly down the midline. Using a drill, a 2 mm craniotomy was made on the right hemisphere anterior to the coronal suture. A 10 μl Hamilton syringe was positioned to inject tumor cells intra-parenchymally into the right hemisphere at a 2.5 mm depth, and 1.5 mm to the right and at 1.0 mm anterior of the bregma. Cells ($3x10^4$) 9L were injected intracerebrally in a 5 μl volume. The craniotomy was covered with a film of polyvinyl chloride glued to the surrounding intact bone and the incision was closed with 4-0 silk suture (Ethicon, Somerville, NJ).

Laser treatment protocol. Rats were injected (i.p.) with the selected doses of Photofrin one day before laser treatment. Photofrin was dissolved in 5% dextrose to a concentration of 12.5 mg/ml. Twenty-four hours after Photofrin administration, the animals were anesthetized i.m. with ketamine (80 mg/kg) and xylazine (13 mg/kg). During treatment, the animal body temperature was monitored using a rectal probe and the temperature was maintained by using a water recirculating K-module. Laser light was administered onto the dura via a craniotomy after removal of the PVC film. An argon-pumped dye laser (Coherent Radiation, Palo Alto, CA) was utilized as the light source at a wavelength of 632 nm, with the optical power density to the dural surface maintained at 50 mW/cm^2 (3 mW laser output). The animals were treated with specified energy fluence. The laser power output and stability was measured before and after treatment, using a photodyne radiometer/photometer power meter.

Behavioral testing

Forelimb-use asymmetry test. Asymmetrical forelimb use was measured by placing rats in a transparent cylinder 30 cm high and with a 20 cm diameter, and recording their behavior when they were rearing and using their forelimbs for weight bearing or when weight shifting along the wall of the cylinder. Twenty consecutive behaviors were analyzed and the asymmetry score was calculated as the number of ipsilateral (unaffected) limb usages (independent of simultaneous use or of alternating (stepping) use with the contralateral forelimb) plus 1/2 the number of 'both' limb usages divided by the total number of limb-use behaviors. The total limb-use number was limited to 20 to prevent habituation. If there was no deficit, the score was ~50%. Higher scores (>50%) indicated greater behavioral deficits.

Somatosensory asymmetry test. Small adhesive dots (Avery adhesive-backed labels, 113 mm^2) were applied to the distal-radial aspect of each forelimb, and the rat was placed back into its home cage. The forelimb that contacted first (i.e., left or right) was recorded in each of 4 trials. If the adhesive stimulus on one particular side was contacted first on 75% or more of the trials, thus indicating that the rat showed a preference for removing the stimulus from that forelimb, then additional tests were conducted to determine the magnitude of the somatosensory asymmetry. The size of the non-preferred limb stimulus was progressively increased, while at the same time the size of the preferred limb stimulus was decreased by an equal amount (14.1 mm^2). When the size of the dot on the non-preferred limb was sufficiently larger than that on the preferred limb, the animal would reverse the original order of contact and the preference was considered to be neutralized. A score was given to reflect this neutralization point. Higher scores represented greater behavioral deficits.

Vibrissae-evoked forelimb placing test. The rat was gently held with one forelimb hanging freely. A same-side placing reaction was elicited by brushing the ipsilateral vibrissae on the corner edge of a countertop. The rat responded by placing its forelimb on the table top while the untested forelimb was kept from placing by the experimenter using gentle pressure on the front of the limb. Similarly, a cross-midline placing response was induced by turning the rat sideways and brushing its contralateral vibrissae against the surface of the table, thus eliciting a placing response in the opposite forelimb. A score was given indicating the percent of successful placing responses during 10 trials for both forelimbs in either of these two placing tests.

Raw scores from the four behavioral tests were transformed to make all the testing outcomes consistent with higher scores indicating greater functional deficits, and they were then standardized with the following formula:

$$y^*_{i,k} = \frac{y_{i,k} - \bar{y}_k}{\sigma^n_k}$$

where $\bar{y}_k$ is the mean and σ^n_k is the standard deviation of $y_{i,k}$ = 1, 2,…, n. Composite scores were produced by summing the four standardized behavioral scores and then adding 4 to avoid the occurrence of negative numbers (15,16).

Single immunohistochemical staining. Brain coronal sections were employed to detect the specific proteins of interest in this project. Sections were incubated with the primary antibodies for the cell type specific proteins; subsequently, the sections were treated with an avidin-biotin complex kit (ABC kit, Vector Laboratories, Inc., Burlingame, CA). Controls used nonimmune serum for the primary antibody or omission of the primary antibodies. Immunohistochemical assessments were performed by an investigator blinded to the experimental groups.

MTT assay for cell viability. The effect of atorvastatin on cell viability was determined by the MTT assay (thiazolyl blue tetrazolium bromide; Sigma). Briefly, cells in an exponential

phase of growth were harvested and seeded in 96-well plates at a density of 10^4 cells per well, and cultured for 24 or 72 h at 37˚C with 5% CO_2. At the end of the culture, the medium in each well was substituted with 200 μl of fresh medium containing MTT (final concentration, 250 μg/ml). Plates were then incubated for an additional 2 h period at 37˚C. Subsequently, the medium was carefully removed in such a way that no loosely adherent cells were removed. Cells containing the trapped MTT crystals were then solubilized in 200 μl DMSO at 37˚C for 15 min. Absorbance was determined in a microtiter plate reader (EL340 Bio-Tek Instruments, Hopkinton, MA) at 570 nm and subtracted from the absorbance at 450 nm. All determinations were performed in quadruplicate and each experiment was repeated at least three times.

Histopathology. Anesthetized animals were sacrificed and perfused with 4% paraformaldehyde. Brains were removed, post-fixed and cut into 1-mm-thick blocks which were then processed and embedded in paraffin. Sections of 6-μm were further cut from each of the blocks containing the tumor and were used for hematoxylin and eosin (H&E) staining and other immunohistochemical stainings.

Histological study of glioma growth and PDT-induced lesions in the brain. To examine the tumor volumes and the PDT-induced brain lesion, the paraffin sections were stained with H&E for light microscopic examination and image analysis. The volume of the tumor tissue and of the lesion in the brain was measured using light microscopic analysis and a Global Lab Image analysis program (Data Translation, Malboro, MA). Each H&E section was evaluated at x2.5 magnification. In each coronal section, the area of the tumor was measured by tracing the demarcation of the lesion by computer, and the volumes (mm^3) were determined by multiplying the appropriate area by the section interval thickness. In the tumored brain, dark purple tumor masses are clearly identified on paraffin sections stained with H&E.

Fluorescence of vascular structure and tumor in cerebral tissue. Using 2D imaging of vibratome sections, the vascular structure in the rat brain was examined. Normal Fischer rats were treated with Photofrin PDT only or Photofrin PDT plus atorvastatin. Animals were perfused with FITC-dextran and sacrificed at 14 days after PDT treatment. Coronal sections at 100 μm intervals were digitized under a 4X objective (Olympus BX40) using a 3-CCD color video camera (Sony DXC-970MD) interfaced with the MCID image analysis system (17).

Three-dimensional image acquisition and analysis. To examine dynamic changes in cerebral blood vessels, we performed three-dimensional morphologic analysis of vessels in the PDT-treated area of the rat brain. Our 3D quantitative analysis program has features to measure number of vessels, number of branch points, segment lengths, and vessel diameters (18-20). The vibratome sections were analyzed with a Bio-Rad MRC-1024 (argon and krypton) laser-scanning confocal microscopy (LSCM) imaging system mounted onto a Zeiss microscope (Bio-Rad, Cambridge, MA), as previously described (17,21). Briefly, a series of 100-μm coronal sections were selected from the beginning to the end of tumor microvessels. Every 5th coronal section per rat was selected for 3D image analyses. Three fields were scanned in the x-y 512x512 pixel (279x279 μm^2) format in the direction using a 4X frame-scan average and twenty-five optical sections along the z-axis with a 1 μm step-size were acquired under a 40X objective. The number of vascular branch points, segment lengths and vessel diameters were measured. The vasculature was identified in 3D analysis by increases in mean vessel diameter and number of vessel branch points, coincident with a decrease in mean vessel length.

Immunohistochemistry and quantification. Antibodies against the vascular endothelial growth factor (VEGF), the von Willebrand factor (vWF) and synaptophysin (Santa Cruz Biotechnology, Santa Cruz, CA, USA) were used to examine their respective expression. A series of 6-μm sections at 50-μm intervals were cut from the block containing the maximum cross-sectional tumor area. After dehydration, sections were boiled in 1% citric acid buffer (pH 6.0) for 10 min, and cooled down to room temperature. The sections were then incubated with 1% BSA to block the non-specific signals, followed by incubation with the primary antibody overnight at 4˚C, and subsequent incubation with a biotinylated secondary antibody for 1 h at room temperature. The reagent 3,3'-diaminobenzidine-tetrahydrochloride (DAB; Sigma) was used to detect the immunoreactivity, which could be directly visualized by bright-field light. Four fields of view from PDT-treated and contralateral hemisphere areas in each section were digitized under a 40X objective (Olympus BX40) using a 3-CCD color video camera (Sony DXC-970MD), interfaced with an MCID image analysis system (Imaging Research, St. Catharines, ON, Canada). Eight fields of view from the tumor were analyzed under the same procedure. The quantitative data are presented as the total number of the immunoreactive cells or the positive area within each field.

Statistical analysis. Data are presented as the mean ± SE. The statistical significance was analyzed by one-way ANOVA. P-values <0.05 are considered statistically significant.

Results

Histological studies of Photofrin-mediated PDT-induced damage to normal brain tissue in rats. We investigated the response of the normal brain to Photofrin-mediated PDT. Normal Fischer rats without tumor were subjected to PDT. H&E staining revealed substantial necrosis (green arrow), patchy hemorrhaging (black arrow), and vacuolization in the lesion area (Fig. 1).

PDT induces behavioral deficits and atorvastatin promotes functional recovery after PDT. We assessed the behavioral responses of normal rats to PDT and the effects of atorvastatin on the functional recovery after PDT treatment. A total of 18 Fischer rats received 2 mg/kg Photofrin i.p. injections, followed by laser exposure at an optical dose of 280 J/cm^2 at 24 h after Photofrin administration. Nine of the PDT-treated animals were treated with 3 mg/kg atorvastatin orally (p.o.) starting at 24 h after laser delivery, daily for 14 days. Nine other PDT-treated animals received the same amount of saline. Control

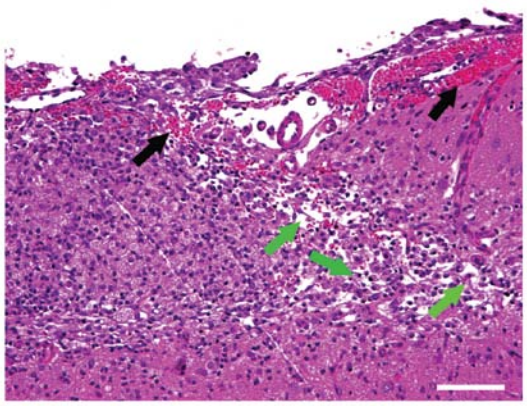

Figure 1. Photofrin-mediated PDT induces damage to normal brain. Image from a representative brain 3 days after PDT at an optical dose of 280 J/cm^2 with 2 mg/kg Photofrin as the sensitizer, stained by H&E. H&E staining revealed substantial necrosis (green arrow), patchy hemorrhage (black arrow), and vacuolization in the lesion area. Scale bar, 100 μm.

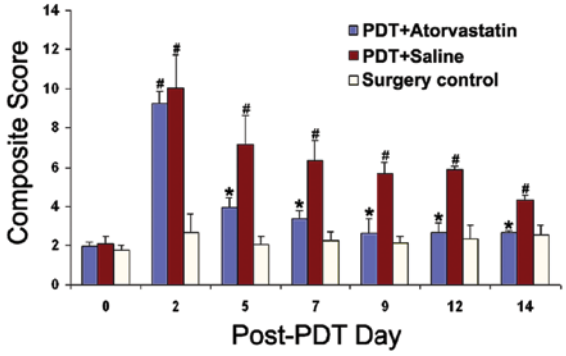

Figure 2. PDT induces functional deficits in normal rats and atorvastatin can promote functional recovery after PDT. Normal animals undergoing PDT exhibited significant behavioral deficits on Days 2, 5, 7, 9, 12 and 14 (P<0.05) after PDT, compared with surgery controls. PDT-treated animals receiving atorvastatin displayed significantly ameliorated behavioral deficits on Days 5, 7, 9, 12 and 14 after PDT (P<0.01), compared to those without atorvastatin administration. $^{\#}$P<0.05 vs. surgery control; *P<0.05 vs. PDT only.

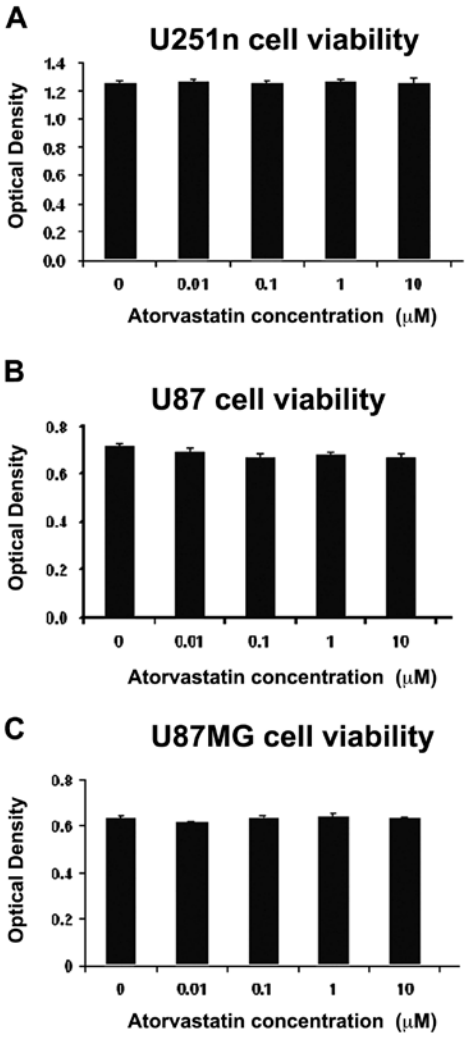

Figure 3. Atorvastatin does not increase glioma cell proliferation *in vitro*. MTT cell proliferation assay demonstrates that atorvastatin at various concentrations did not significantly increase the viability of U251n (A), U87 (B) and U87MG (C) glioma cells. Data are presented as mean ± SE.

animals (n=9) underwent the same surgical procedure, including the removal of the skull, but did not receive Photofrin and laser treatment. Functional measures were carried out before and after PDT dynamically, using sensitive behavioral tests including the forelimb-use asymmetry test, somatosensory asymmetry test, same-side placing test and cross-midline placing test. Composite scores were produced by summing the 4 standardized behavioral scores and then adding 4 to avoid the occurrence of negative numbers (15,16). Our data show that normal animals undergoing PDT exhibited significant behavioral deficits on Days 2, 5, 7, 9, 12, and 14 (P<0.05) after PDT treatment, compared with surgery controls. PDT-treated animals receiving atorvastatin displayed significantly ameliorated behavioral deficits on Days 5, 7, 9, 12, and 14 after PDT (P<0.01), compared to those without atorvastatin administration (Fig. 2). All animals were sacrificed 14 days after treatment and PDT induced lesion volumes were measured. No significant differences in PDT lesion volumes were detected between the atorvastatin-treated and the non-treated groups (32.36±6.15 mm^3 vs. 33.49±5.74 mm^3, respectively). These results suggest that PDT, though an effective anticancer treatment, can itself induce functional deficits, and atorvastatin treatment promotes functional restoration after PDT.

Atorvastatin does not promote glioma growth and does not diminish the glioma response to PDT. The effects of atorvastatin on glioma cell growth were examined *in vitro* and *in vivo*. Three different human origin glioma cell lines U251, U87 and U87MG were employed. Cell viability was determined by the MTT cell proliferation assay. Our data show that atorvastatin did not affect the growth of U251n, U87 and U87MG glioma cells (Fig. 3). In another experiment, Fischer rats with intracranial 7-day-old 9L glioma were randomly subjected to no treatment, PDT alone (Photofrin, 12.5 mg/kg; optical dose, 140 J/cm^2), atorvastatin alone (10 mg/kg s.c., daily until sacrificed), or atorvastatin (10 mg/kg s.c., daily until sacrifice) combined with 12.5 mg/kg Photofrin at an optical dose of 140 J/cm^2. All animals (6 nude rats/each group) were sacrificed on Day 14 after tumor implantation and the tumor volume was evaluated (Fig. 4). Histological data demonstrate that atorvastatin did not promote tumor growth *in vitro* and *in vivo*.

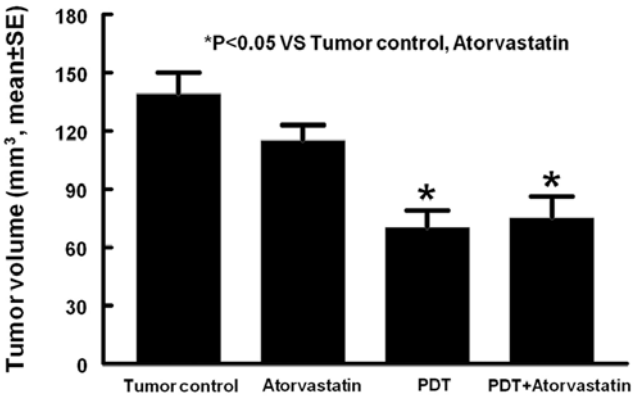

Figure 4. Tumor volumes in different groups. Tumor volume was significantly reduced by PDT with or without atorvastatin treatment. Atorvastatin did not increase 9L tumor growth.

Additionally, atorvastatin did not diminish the glioma response to PDT.

Atorvastatin administration reduces the PDT-induced damage in astrocytes and endothelial cells in vitro. The MTT assay was employed to test the effect of atorvastatin (0.001 μmol/l) on the viability of astrocytes and endothelial cells after PDT *in vitro*. Our data show that PDT (Photofrin, 5 μg/ml, optical dose, 180 J/cm^2) significantly decreased astrocyte and endothelial cell proliferation. However, atorvastatin significantly reduced the cell damage caused by PDT (Fig. 5). In astrocytes, PDT significantly decreased cell viability by 63.1±6.5% (P<0.01); atorvastatin administration significantly increased astrocyte cell viability by 49.7±18.1%, compared to PDT alone. Similarly, in endothelial cells, PDT significantly decreased cell viability by 24.3±13.1% (P<0.01); atorvastatin administration significantly increased astrocyte cell viability by 27.6±7.1%, compared to PDT alone.

Atorvastatin induces vascular density in the PDT-damaged Fischer rat brain. Vascular structures in the normal brain (9 animals/group) were examined in Fischer rats after PDT and atorvastatin treatment. PDT treatment induced abnormal vascular structures in the PDT-damaged brain tissue that were visible to the naked eye and can be described and identified as regions of low vessel density, with increased broken vascular structures. However, atorvastatin administration provided significant recovery of the vascular structures (Fig. 6). For 3-D analysis, vibratome sections were analyzed with a laser-scanning confocal imaging system mounted onto a Zeiss microscope. Using software developed in our laboratory (22), abnormal vasculature was identified by a significant decrease in the number of vessel branch points, coincident with a significant increase in mean vessel length, and decreased mean vessel diameter. Reconstructed 3-D cerebral microvessels (Fig. 7) of PDT plus atorvastatin treatment (Fig. 7A and C), and PDT-treated area (Fig. 7B and D) data, indicate that atorvastatin treatment leads to a quantifiable recovery in the vascular structure of the PDT-damaged tissue (Fig. 7E).

Atorvastatin induces VEGF, vWF and synaptophysin in the PDT-damaged brain tissue. To further assess the mechanisms of the neurorestorative effects of atorvastatin on the PDT-damaged brain, immunohistochemistry was employed to measure the expression of angiogenesis and synaptogenesis factors after PDT and atorvastatin treatment in Fischer rats. Eight fields of view from the tumor were analyzed. Expression of VEGF, and synaptophysin were analyzed and the data are presented as the percentage of the immunoreactive area in the field. Expression of the vWF was analyzed and data are presented as the number of vWF-positive vessels/mm^2. Both VEGF and vWF as well as synaptophysin immunoreactivity were significantly (P<0.05) increased in the PDT-damaged mouse brain treated with PDT plus atorvastatin compared with the immunoreactivity in the brain of animals treated with PDT alone (Fig. 8). VEGF, vWF and synaptophysin

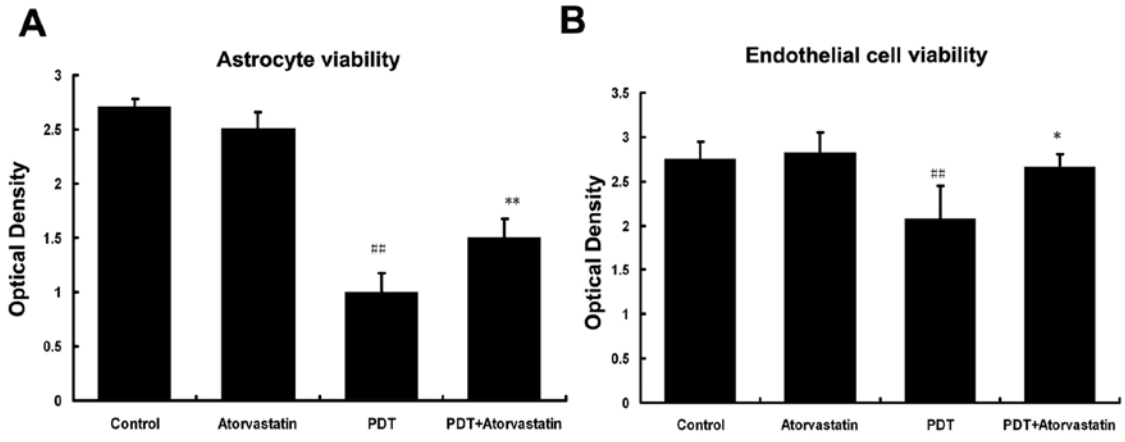

Figure 5. Effect of atorvastatin on PDT-induced cytotoxicity in astrocytes and mouse brain endothelial cells *in vitro*. Astrocytes and brain endothelial cells were treated with PDT with and without atorvastatin. At 24 h after treatment, astrocytes and endothelial cells were subject to the MTT assay. Panels A and B show the quantification data of the cell viability MTT assay in astrocytes (A) and brain endothelial cells (B), respectively. Data are presented as mean ± SE. Atorvastatin treatment significantly decreased cytotoxicity induced by PDT in both of these cells. Also, atorvastatin had no significant effect on cell viability as compared to control. ##Indicates a significant difference between the PDT-treated group and controls (P<0.01). *Indicates a significant difference between PDT receiving atorvastatin and without atorvastatin (P<0.05). **Indicates a significant difference between PDT receiving atorvastatin and without atorvastatin (P<0.01).

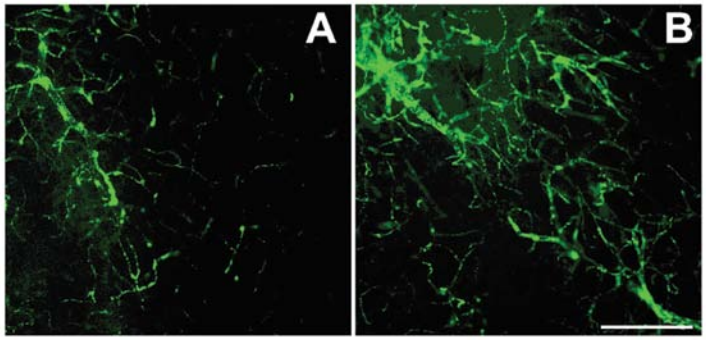

Figure 6. 2D images of FITC-dextran perfused vessels. Normal Fischer rats were treated with Photofrin PDT only or Photofrin PDT plus atorvastatin treatment. Animals were perfused with FITC-dextran and sacrificed 14 days after PDT treatment. This image shows a representative coronal section of FITC-dextran perfused vessels within the PDT treated area from the rats treated with PDT only (A), and from the rats treated with PDT plus atorvastatin (B). Scale bar, 100 μm. The data shows that PDT significantly alters the vasculature within the treated area, and this PDT-induced abnormal vessel density and abnormal vasculature are significantly reduced by the atorvastatin therapy.

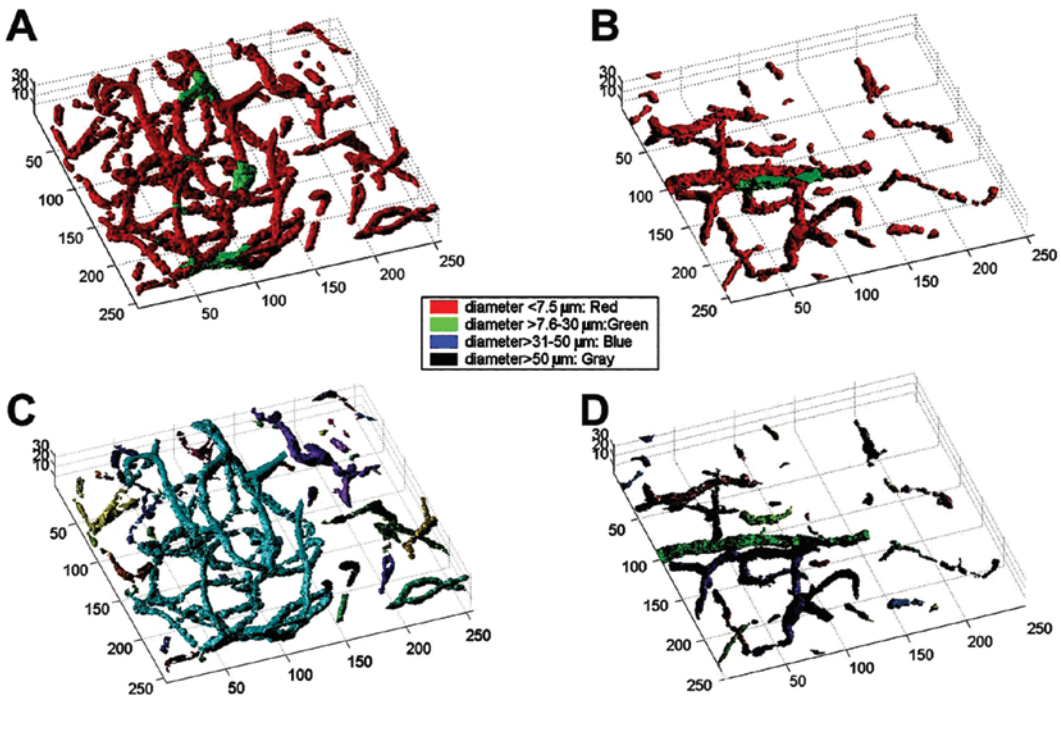

E

	Normal rats control	PDT–treated rats	PDT plus Atorvastatin–treated rats
Length (µm) ± SE	37.5±2.8	49.8±2.7	41.6±1.7
Number of branch points ± SE	28.4± 2.4	11.3±2.1	23.8 ±2.6

Figure 7. Reconstructed 3D images derived from the original images obtained from Laser scanning confocal microscopy of FITC-dextran perfused vessels in normal brain after PDT treatment. Panels A and C were obtained from the hemisphere ipsilateral to PDT and atorvastatin treatment, and panels B and D were obtained from the hemisphere ipsilateral to PDT. Panels A-D, 3D images of color-coding highlights vessel diameters (A and B) and connectivity (C and D), respectively. Decreased vessel density within the PDT-treated hemisphere is evident. Quantitative data (E) on the length of vessels and branch points obtained from the rats under different treatments. The length of vessels is significant increased, and the number of vessel branch points is significantly decreased in the PDT-treated brain compared to normal control groups. However, the PDT-induced abnormal vessel structures are significantly recovered in the PDT plus atorvastatin group.

expression increased from 3.6±0.6 to 7.3±0.8, 207.1±21.3 to 315.3±34.7, 13.27±2.63% to 23.0±2.9%, respectively, in the atorvastatin-treated animals compared to the PDT-only treatment group. The data demonstrate that atorvastatin induces angiogenesis and synaptogenesis in the PDT-damaged brain tissue.

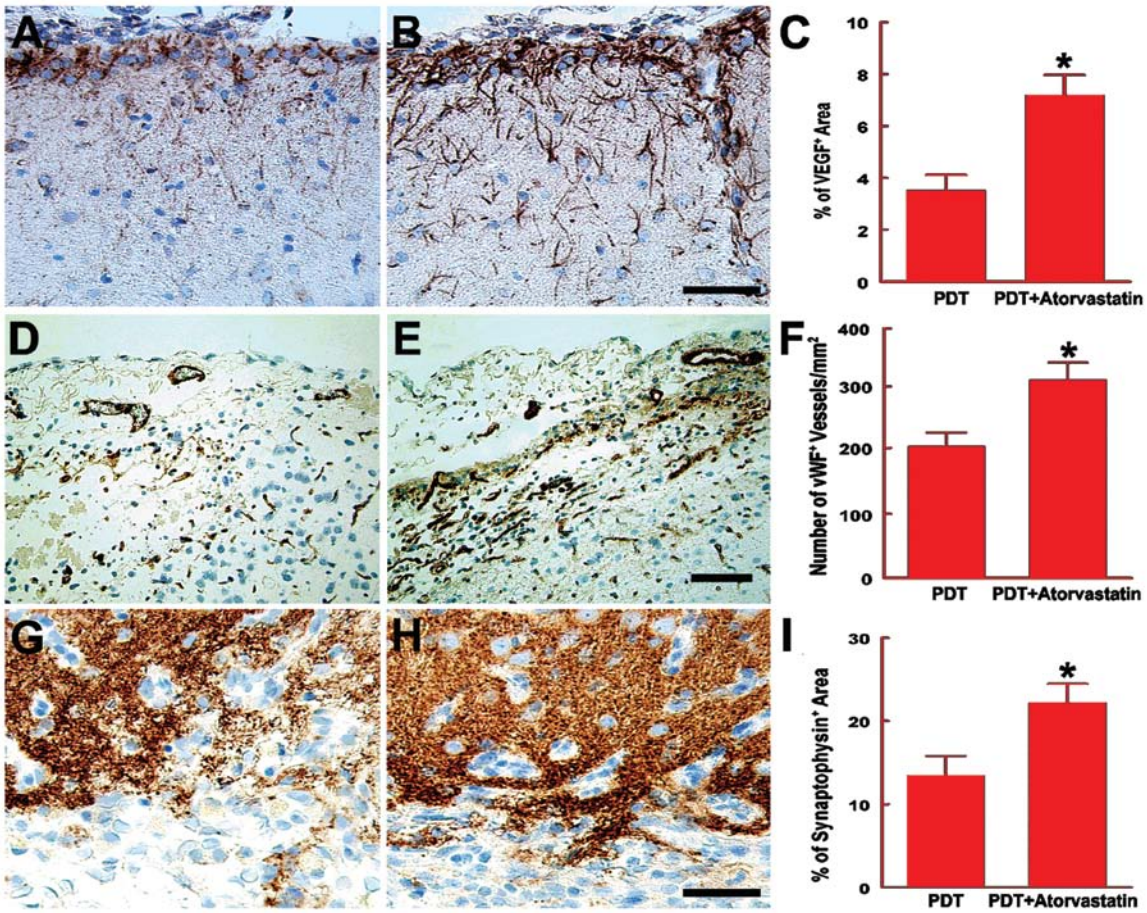

Figure 8. Atorvastatin induces VEGF, vWF and synaptophysin expression in the PDT-damaged brain tissue. VEGF, vWF and synaptophysin are expressed in the PDT induced lesion border 14 days after PDT treatment. (A, D and G) VEGF (A), vWF (D) and synaptophysin (G) expression in the PDT-only-treated control rats. (B, E and H) VEGF (B), vWF (E) and synaptophysin (H) expression in representative rats treated with atorvastatin after PDT-induced brain damage. (C, F and I) Quantitative data of VEGF (C), vWF (F) and synaptophysin (I) in the ischemic border area. Data are presented as the mean ± SE. Scale bars, 100 μm.

Discussion

Brain tumors are distinguished from other tumors by the fact that every brain area has an associated function, and the tumors arise in the skull with little room for expansion. Surgery is generally the first step and the most effective treatment for malignant tumors, that reduces the size of the tumor as well as brain pressure. Malignant gliomas are highly invasive, and are characterized by a high incidence of recurrence and poor prognosis (23-25). Aggressive brain tumor treatments, such as extensive surgical resection, tend to enhance tumor destruction and delay tumor recurrence. However, such treatments damage adjacent normal tissue, and thus are not easily attained. Therefore, novel therapeutic strategies aimed at improving the efficacy/toxicity ratio are desperately needed.

Photodynamic therapy (PDT) has been established in the clinical environment as a useful adjuvant to standard treatments for brain tumors. Our previous studies (26) have demonstrated that PDT sacrifices tumor cells in a dose-dependent manner and inhibits brain tumor invasion and recurrence. However, a high dose of PDT treatment results in increased damage to the surrounding normal brain tissue, which may induce functional deficits. Administration of atorvastatin shows neuroprotective effects in the treatment of stroke and other brain injuries (8,12). Therefore atorvastatin may be employed to reduce neurological deficits associated with aggressive tumor treatments such as surgery and high dose of PDT.

In the present study, for the first time, we examined whether PDT causes severe neurological deficits by injuring the normal brain tissue, and whether a widely clinically employed statin, atorvastatin, when administered at a low dose to a PDT-damaged rat evokes significant improvement in functional neurological recovery. Additionally, we tested whether atorvastatin decreases the PDT-induced damage in astrocytes as well as in endothelial cells. We also investigated whether the effects of atorvastatin treatment on the functional recovery in rats followed by aggressive PDT was associated with the induction of angiogenesis and synaptogenesis. We also investigated whether the treatment of atorvastatin would promote tumor growth.

Our results clearly indicate that PDT significantly induces brain damage and behavioral deficits in normal Fischer rats. However, atorvastatin significantly protects the PDT-induced damage in astrocytes and endothelial cells, and promotes functional recovery in rats damaged by the treatment of PDT. Most importantly, treatment with atorvastatin at the dose which provides functional recovery from PDT damage did not promote tumor growth and did not diminish the glioma response to PDT treatment.

PDT damages the brain tissue and normal brain cells such as astrocytes and endothelial cells, and induces significant functional deficits in normal rats. The destruction of both tumor and normal surrounding tissue by PDT is dependent on the laser optical and the photosensitizer doses (26-28). Complete tumor elimination requires an increase in PDT intensity. However, increased PDT intensity leads to increased damage to normal surrounding tissues and aggravated neurological deficits. Therefore, the concern of the functional impairment sets the dose limit of PDT in the clinic.

Our previous studies have demonstrated that chronic administration of atorvastatin reduces neurological deficits induced by brain injury and stroke (8,12). Aggressive PDT may destroy tumor, but inevitably there is damage to normal cerebral tissue which diminishes the patient's neurological function and or reduces survival time. We hypothesize that atorvastatin administration reduces the damage caused by aggressive PDT treatment, and thereby enhance and prolong the quality of the patient's life after treatment. Adjuvant atorvastatin treatment would possibly also make aggressive PDT treatment clinically applicable, since our data demonstrate that the brain injury induced by PDT could be significantly counteracted by atorvastatin treatment.

PDT elicits both apoptotic and necrotic responses within brain adjacent to tumor (BAT) and produces microvascular injury leading to inflammation and hypoxia. Based on our results, atorvastatin induces a significantly higher microvessel density and increased expression of VEGF in the PDT-damaged brain tissue, suggesting that atorvastatin reduces the neurotoxicity and the functional deficits caused by PDT partly through the promotion of angiogenesis. Angiogenesis in the injured BAT creates a hospitable microenvironment for neuronal plasticity leading to functional recovery.

Synaptic plasticity is also important for re-establishment of function following injury. Atorvastatin administration significantly increases the expression of synaptophysin in the PDT-damaged tissue. This suggests that functional improvement may not only be associated with cellular survival and angiogenesis, but also with structural changes in neurons, including increase in synaptic density.

In this study, we have demonstrated that atorvastatin significantly provides a neuroprotective and a neurorestorative effect to the PDT-damaged brain tissue. However, the key questions for this novel combinational therapeutic approach are: i) if a treatment is beneficial to normal brain tissue, can it also nourish the tumor and promote tumor growth? ii) if a treatment protects normal brain tissue during anticancer therapy, can it also help protect the tumor against the anticancer therapy? iii) if a treatment enhances restoration of damaged brain tissue, can it also stimulate the remaining tumor cells to grow into a tumor? To address these questions, we have shown that atorvastatin does not have a direct mitotic effect on glioma cells and atorvastatin has no effect on 9L tumor growth or viability. Also, atorvastatin does not diminish the glioma response to PDT.

In summary, our study demonstrates that atorvastatin administration significantly reduces PDT evoked neurological deficits. And importantly, atorvastatin administration does not promote tumor growth and does not diminish the glioma response to PDT. Thus, atorvastatin as a neuroprotective and neurorestorative agent may significantly improve brain function after high dose PDT, thus making high dose PDT and possibly other anti-cancer agents applicable to the clinic to enhance glioma therapy.

Acknowledgements

The authors thank Mrs. Cindi Roberts and Qing-e Lu for technical assistance.

References

1. Stylli SS and Kaye AH: Photodynamic therapy of cerebral glioma – A review Part I – A biological basis. J Clin Neurosci 13: 615-625, 2006.
2. Stylli SS and Kaye AH: Photodynamic therapy of cerebral glioma – A review. Part II – Clinical studies. J Clin Neurosci 13: 709-717, 2006.
3. Hanlon JG, Adams K, Rainbow AJ, Gupta RS and Singh G: Induction of Hsp60 by Photofrin-mediated photodynamic therapy. J Photochem Photobiol B 64: 55-61, 2001.
4. Evans S, Matthews W, Perry R, Fraker D, Norton J and Pass HI: Effect of photodynamic therapy on tumor necrosis factor production by murine macrophages. J Natl Cancer Inst 82: 34-39, 1990.
5. Gollnick SO, Evans SS, Baumann H, *et al*: Role of cytokines in photodynamic therapy-induced local and systemic inflammation. Br J Cancer 88: 1772-1779, 2003.
6. Gollnick SO, Liu X, Owczarczak B, Musser DA and Henderson BW: Altered expression of interleukin 6 and interleukin 10 as a result of photodynamic therapy in vivo. Cancer Res 57: 3904-3909, 1997.
7. Nseyo UO, Whalen RK, Duncan MR, Berman B and Lundahl SL: Urinary cytokines following photodynamic therapy for bladder cancer. A preliminary report. Urology 36: 167-171, 1990.
8. Chen J, Zhang ZG, Li Y, *et al*: Statins induce angiogenesis, neurogenesis, and synaptogenesis after stroke. Ann Neurol 53: 743-751, 2003.
9. Chen J, Zhang C, Jiang H, *et al*: Atorvastatin induction of VEGF and BDNF promotes brain plasticity after stroke in mice. J Cereb Blood Flow Metab 25: 281-290, 2005.
10. Seyfried D, Han Y, Lu D, Chen J, Bydon A and Chopp M: Improvement in neurological outcome after administration of atorvastatin following experimental intracerebral hemorrhage in rats. J Neurosurg 101: 104-107, 2004.
11. Lu D, Mahmood A, Qu C, Goussev A, Lu M and Chopp M: Atorvastatin reduction of intracranial hematoma volume in rats subjected to controlled cortical impact. J Neurosurg 101: 822-825, 2004.
12. Lu D, Goussev A, Chen J, *et al*: Atorvastatin reduces neurological deficit and increases synaptogenesis, angiogenesis, and neuronal survival in rats subjected to traumatic brain injury. J Neurotrauma 21: 21-32, 2004.
13. Lu D, Mahmood A, Goussev A, *et al*: Atorvastatin reduction of intravascular thrombosis, increase in cerebral microvascular patency and integrity, and enhancement of spatial learning in rats subjected to traumatic brain injury. J Neurosurg 101: 813-821, 2004.
14. Lu D, Mahmood A, Goussev A, Qu C, Zhang ZG and Chopp M: Delayed thrombosis after traumatic brain injury in rats. J Neurotrauma 21: 1756-1766, 2004.
15. Schallert T and Lindner MD: Rescuing neurons from transsynaptic degeneration after brain damage: helpful, harmful, or neutral in recovery of function? Can J Psychol 44: 276-292, 1990.
16. Lu M, Chen J, Lu D, Yi L, Mahmood A and Chopp M: Global test statistics for treatment effect of stroke and traumatic brain injury in rats with administration of bone marrow stromal cells. J Neurosci Methods 128: 183-190, 2003.
17. Zhang X, Zheng X, Jiang F, Zhang ZG, Katakowski M and Chopp M: Dual-color fluorescence imaging in a nude mouse orthotopic glioma model. J Neurosci Methods 181: 178-185, 2009.
18. Zhang ZG, Zhang L, Tsang W, *et al*: Correlation of VEGF and angiopoietin expression with disruption of blood-brain barrier and angiogenesis after focal cerebral ischemia. J Cereb Blood Flow Metab 22: 379-392, 2002.

19. del Zoppo GJ: Microvascular changes during cerebral ischemia and reperfusion. Cerebrovasc Brain Metab Rev 6: 47-96, 1994.
20. Jiang F, Zhang X, Kalkanis SN, *et al*: Combination therapy with antiangiogenic treatment and photodynamic therapy for the nude mouse bearing U87 glioblastoma. Photochem Photobiol 84: 128-137, 2008.
21. Zhang ZG, Chopp M, Goussev A, *et al*: Cerebral microvascular obstruction by fibrin is associated with upregulation of PAI-1 acutely after onset of focal embolic ischemia in rats. J Neurosci 19: 10898-10907, 1999.
22. Jiang F, Zhang Z, Kalkanis S, *et al*: A quantitative model of tumor-induced angiogenesis in the nude mouse. Neurosurgery 57: 320-324, 2005.
23. Burger PC and Kleihues P: Cytologic composition of the untreated glioblastoma with implications for evaluation of needle biopsies. Cancer 63: 2014-2023, 1989.
24. Kleihues P, Louis DN, Scheithauer BW, *et al*: The WHO classification of tumors of the nervous system. J Neuropathol Exp Neurol 61: 215-226, 2002.
25. Nicholas MK, Prados MD and Larson DA: Malignant Astrocytomas. In: Cancer of the Nervous System. Black PM, Loeffler JS (eds). Blackwell, London, pp464-491, 1997.
26. Chopp M, Dereski MO, Madigan L, Jiang F and Logie B: Sensitivity of 9L gliosarcomas to photodynamic therapy. Radiat Res 146: 461-465, 1996.
27. Chopp M, Madigan L, Dereski M, Jiang F and Li Y: Photodynamic therapy of human glioma (U87) in the nude rat. Photochem Photobiol 64: 707-711, 1996.
28. Krishnamurthy S, Powers SK, Witmer P and Brown T: Optimal light dose for interstitial photodynamic therapy in treatment for malignant brain tumors. Lasers Surg Med 27: 224-234, 2000.